The role of the double-well potential seen by the amino group in the ferroelectric phase transition in triglycine sulfate

The role of the double-well potential seen by the amino group in the ferroelectric phase transition in triglycine sulfate

Rajul Ranjan Choudhury, R Chitra and M Ramanadham

Solid State Physics Division, Bhabha Atomic Research Centre, Mumbai 400085, India

E-mail: rajul-ranjan@indiatimes.com

Abstract
The two most important molecular movements which bring about the order–disorder ferroelectric phase transition in the hydrogen-bonded ferroelectric triglycine sulfate (TGS) are the swinging of the amino group ($-NH_3^+$) of one of its three glycine ions, namely GI, and the tunnelling of hydrogen in the hydrogen bond between its other two glycine ions, GII and GIII (GII–H–GIII). The potential function for bent hydrogen bonds is used along with the structural parameters of the TGS crystal to model the double-well potential (U) seen by the amino group ($-NH_3^+$) of GI in TGS. The ferroelectric phase transition in TGS is investigated from the point of view of the double-well instability. Results obtained are in good agreement with those obtained earlier using the Ising-type theoretical model. Correlation between the two crucial molecular movements in TGS, namely swinging of the $-NH_3^+$ group of GI and tunnelling of hydrogen in the hydrogen bond GII–H–GIII of TGS, is established.

1. Introduction

Triglycine sulfate (TGS) belongs to a family of hydrogen-bonded ferroelectrics that has been extensively studied using various techniques [1–3], including single-crystal neutron diffraction [4]. Its use as an infrared radiation detector stems from its pyroelectric property [5, 6]. TGS undergoes a second-order, order–disorder type ferroelectric phase transition at 322 K (T_C). The crystal structure of TGS belongs to the monoclinic system in both ferroelectric and paraelectric phases, with the space groups being $P2_1$ and $P2_1/m$ below and above the transition temperature respectively [7]. An asymmetric unit of the TGS unit cell contains three glycine ions (GI, GII and GIII) and a sulfate ion (figure 1). GI and the sulfate ion lie closer to the crystallographic ac-plane (MP) that intersects the crystallographic b-axis at $0.25b$ (at $0.75b$ in the second asymmetric unit). This plane (MP) becomes the mirror plane
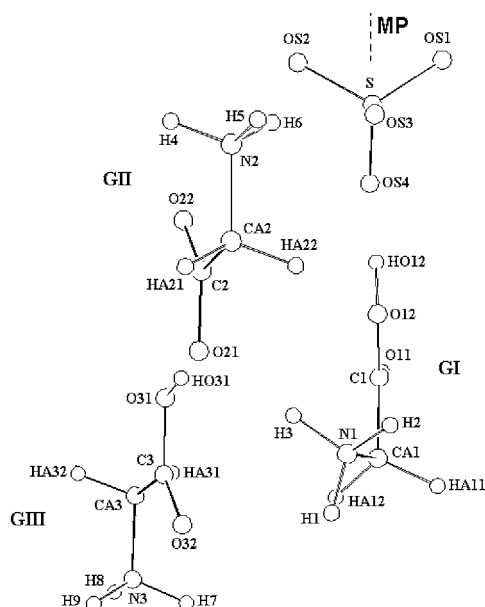
Figure 1. An asymmetric unit of the TGS unit cell.

in the paraelectric phase. GII and GIII are linked through a short hydrogen bond (GII–H–GIII) between their carboxyl groups (figure 1).

In the ferroelectric phase of TGS the amino group of GI has two [3] equivalent positions labelled L and R in figure 2(a) on either side of MP, corresponding to the two spontaneous polarization directions of TGS. In the unit cells of one of the two ferroelectric domains of TGS the hydrogen in the GII–H–GIII hydrogen bond is covalently linked to GIII; in the alternate domain it is covalently linked to GII. At the time of polarization switching in the ferroelectric phase [8] the amino group of GI and the proton in the hydrogen bond GII–H–GIII move between their two equivalent positions; from the spectroscopic studies conducted on TGS [9] it was concluded that these two molecular movements of TGS are coupled although the exact nature of coupling between the two was not established. These two movements become completely disordered in the paraelectric phase, making the plane MP a mirror plane (in the statistical sense) of the space group $P2_1/m$ [7]. Various experimental investigations [3, 9] have demonstrated that the amino group of GI and the hydrogen bond (GII–H–GIII) between the carboxyl groups of GII and GIII are the two contributing factors to the ferroelectric phase transition of TGS. The transition temperature of deuterated TGS is 334 K, only 12 K more than that of undeuterated TGS, unlike the hydrogen-bonded ferroelectric KDP where the difference between the transition temperatures of deuterated and undeuterated samples is much larger ($\sim$107 K). The significant change in the transition temperature of KDP on deuteration is attributed to the changes in its hydrogen bond geometry on deuteration [10]; similar changes take place in the GII–H–GIII hydrogen bond geometry in TGS on deuteration but still the change in its T_C on deuteration is not that drastic. This fact indicates that, unlike the ferroelectric phase transition in KDP [11], the proton tunnelling in the hydrogen bond GII–H–GIII is not the primary driving force of the phase transition in TGS. It is generally believed that the dynamics of the amino group ($-NH_3^+$) of GI initiates the phase transition [3], though one can make a quantitative statement about the relative importance of these two motions only after conducting a dynamics experiment.
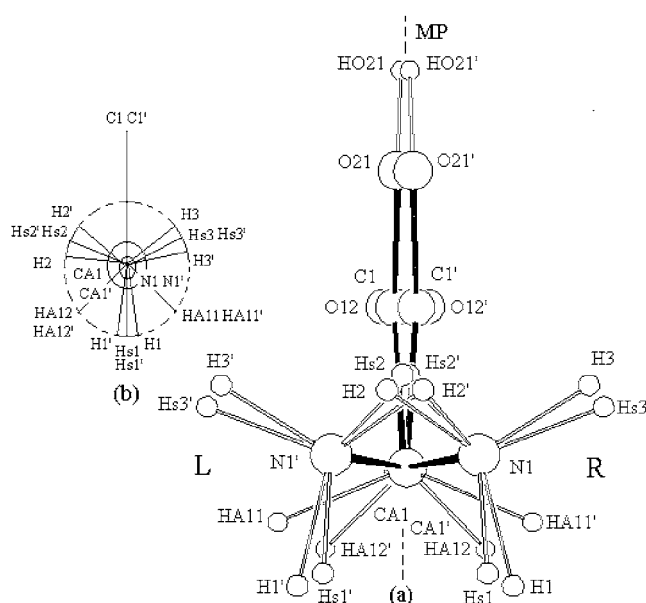
Figure 2. (a) Two positions L and R of the amino group of GI about the plane MP. (Primed labels are for the L position.) (b) Conformational reorientation of the hydrogen atoms of the amino group: Hs1, Hs2, Hs3, Hs1′, Hs2′ and Hs3′ are the hydrogen positions for the staggered conformation.

NMR studies conducted [3] on TGS gave the correlation time for the flipping of $-NH_3^+$ in the paraelectric phase as $\tau_f = 1.2 \times 10^{-11}$ s. The Raman studies conducted earlier [12] have shown that the amino group of GI experiences a double-minimum potential; this paper attempts to model this double-minimum potential using the structural information of TGS. Using this potential the ferroelectric phase transition in TGS is interpreted in terms of the dipolar interaction energy between the amino-group orientations. An attempt is made to find the nature of coupling between the swing of the amino group and the proton tunnelling in the hydrogen bond GII–H–GIII using the hydrogen bonding propensities of carboxyl groups.

2. Modelling of potential experienced by the amino group in GI

In one of the two ferroelectric domains of TGS, the amino group of GI is at one extreme position L with respect to the plane MP, while most of the other non-hydrogen atoms of GI are very close but on the other side of this plane (figure 2(a)). The situation is reversed in the second domain (figure 2(a)); it is clear from figure 2(a) that the amino group undergoes maximum displacement during polarization reversal. The net swing between the two extremes of the amino group is about 43°. In addition, the three hydrogen atoms of the amino group at L are rotated around the CA1–N1 bond by about 10° from the ideal staggered conformation (figure 2(a)). This happens to optimize the hydrogen bond geometry involving these hydrogen atoms (hence, minimize the hydrogen bond energy). This conformational change is in the opposite sense, but by the same amount in the other extreme orientation R of the amino group (figure 2(a)). Thus, there is a maximum 20° of conformational reorientation of the hydrogen atoms of this amino group about the staggered conformation as the group moves between the two extreme orientations (figure 2(b)).

In the analysis, coordinates of the nitrogen atom and the three hydrogen atoms of the amino group of GI at the intermediate positions as the group moves from the R position to the L position
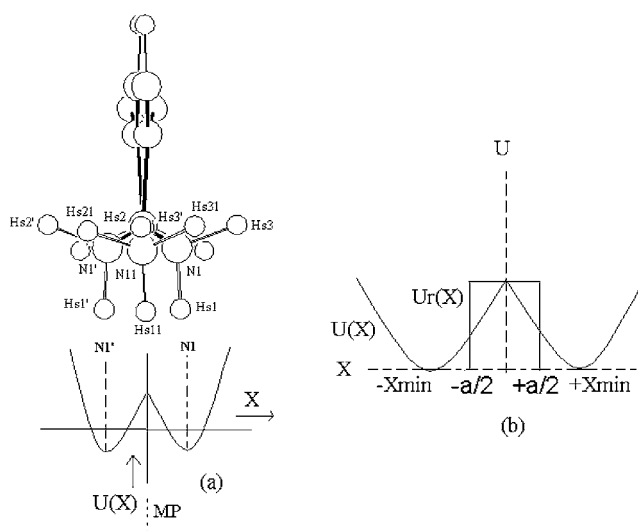
Figure 3. (a) Different orientations of the amino group as it moves from the L to the R position. (b) Rectangular approximation of the potential barrier seen by the amino group.

were generated; movements of the other non-hydrogen atoms of GI were neglected as they were an order of magnitude smaller than the amino group movement. Starting from the atomic coordinates taken from the single-crystal neutron diffraction study by Kay and Kleinberg [4], intermediate co-ordinates (N1i) of the nitrogen atom of the group were generated assuming that the nitrogen atom of the group moves along the arc N1–N1$'$ of a circle with its centre at CA1 and radius equal to the CA1–N1 bond length (figure 3(a)). N1 and N1$'$ correspond to the two experimentally obtained nitrogen atom positions of R and L respectively, and N1i for $i = 1, 2, 3, \ldots$ correspond to various intermediate nitrogen positions (figure 3(a)). The co-ordinates of the hydrogen atoms (Hs1i, Hs2i and Hs3i) of the group were generated considering the conformation of the amino group at the various positions to be the staggered (figure 3(a)) conformation, because, as mentioned above, the deviations from the staggered conformation are not very significant (figure 2(b)). The potential as seen by the amino group in its various orientations is computed as described below.

3. Potential function for bent hydrogen bonds

The semi-empirical Lippincott–Schroeder potential function for linear hydrogen bonds was modified earlier by Chidambaram and Sikka [13] to describe the potential energy of bent O–H- - -O hydrogen bonds. This method was later extended to N–H- - -O (with sp^2 hybridized N atom) and N$^+$–H–O (with sp^3 hybridized and protonated N atom) hydrogen bonds [14, 15]. This potential function, V_{HB}, is given by

$$V_{HB} = V_1 + V_2 + V_3 + V_4. \tag{1}$$

$V_1 = D_1\{1 - \exp(-n_1(r - r_{01})^2/2r)\}$ gives the change in N–H covalent energy due to bond stretching, $V_2 = -CD_2\{\exp(-n_2(d - r_{02})^2/2Cd)\}$ gives the attractive interaction energy between H$^{\delta+}$ and O$^{\delta-}$, $V_3 = A\exp(-b(R - R_{min}))$ gives the N- - -O repulsive non-bonded interaction energy, $V_4 = -B/R^6$ gives the N- - -O attractive non-bonded interaction energy, D_1 and D_2 are the bond dissociation energies and r_{01} and r_{02} are the equilibrium bond distances for N–H and H–O covalent bonds respectively. R, r and d are the N- - -O, N–H and H- - -O

Table 1. Variation of hydrogen bond interaction energies of the three hydrogen bonds N1i–Hs1i- - -Os2, N1i–Hs2i- - -O12 and N1i–Hs3i- - -O21 as the amino group moves away from the equilibrium position R. X is the distance of the group from the ac-plane at $0.25b$.

N1i	V_{HB} (N1i–Hs1i- - -Os2) (kcal mol^{-1})	V_{HB} (N1i–Hs2i- - -O12) (kcal mol^{-1})	V_{HB} (N1i–Hs3i- - -O21) (kcal mol^{-1})	U_{TOTAL} (kcal mol^{-1})	$X = d$ (N11–N1i) (Å)
N12	−2.04	15.22	−2.09	11.09	0.11
N13	−1.77	10.26	−2.65	5.84	0.23
N14	−1.31	3.17	−3.25	−1.38	0.39
N1	−1.32	−1.08	−2.02	−4.42	0.55
N15	−1.09	−2.91	4.22	0.22	0.69
N16	−1.43	−2.99	18.78	14.36	0.82
N17	−1.84	−2.71	35.08	30.53	0.89

distances obtained from the crystal structure, C is a factor less than unity which takes into account the weakness of the H- - -O hydrogen bond relative to a H–O covalent bond at the same separation and $n = kr_0/D$ where k is the force constant for the stretching vibration of the covalent bond. A, B, b and R_{min} are constants dependent on the donor (N) and acceptor (O) atoms. This semi-empirical model explains fairly satisfactorily various properties of hydrogen bonds such as N–H stretching frequency shifts.

The values of constants used in this paper are $D_1 = 104.0$ kcal mol^{-1}, $D_2 = 110.8$ cal mol^{-1}, $r_{01} = 1.014$ Å, $r_{02} = 0.957$ Å, $n_1 = 9.30$ Å^{-1}, $n_2 = 9.06$ Å^{-1}, $C = 0.715$, $A = 5.050$ kcal mol^{-1}, $b = 7.854$ Å^{-1}, $B = 1.812 \times 10^3$ Å^6 kcal mol^{-1} and $R_{min} = 2.83$ Å. The values of potential parameters A, b, R_{min} and B reported by Ramanadham and Chidambaram [15] were used here; these values were obtained after refinement using 74 neutron structures of small molecules having N$^+$–H- - -O hydrogen bonds (neutrons give the hydrogen atom positions most unambiguously).

4. Computation of hydrogen bond energy of −NH$_3^+$ group

At each of the generated −NH$_3^+$ positions, the net hydrogen bond interaction energy of this terminal group due to the hydrogen bonds made by its three hydrogen atoms (N1i^+–Hs1i- - -Os2, N1i^+–Hs2i- - -O12, N1i^+–Hs3i- - -O21) was calculated using the potential function for bent N$^+$–H- - -O bonds described above. Table 1 gives the details of the energy calculation as the group moves away from the equilibrium position R. (X represents the distance of the −NH$_3^+$ group from the plane MP; N11 is the position of nitrogen in the ac-plane.)

The symmetry of the structure about the ac-plane insures that one gets a mirror image of the above potential as the group moves in the $−X$-direction i.e. away from the L position.

As the group moves from the minimum energy position N1 towards the ac-plane the hydrogen bond N1i^+−Hs2i- - -O12 becomes more and more bent and the distance R between the nitrogen donor (N1i) and oxygen acceptor (O12) reduces, resulting in a sharp increase in the repulsive energy V_3 between the two.

Similarly, when the group moves in the opposite direction, away from the ac-plane, the hydrogen bond N1i^+–Hs3i- - -O21 becomes progressively bent, leading to a significant increase in the repulsive energy V_3 between the donor (N1i) and acceptor (O21) due to the decrease in the separation R between the two. Figure 4 shows a plot of U_{TOTAL} against X.

A polynomial of order 4 was fitted to the U_{TOTAL} versus X data, giving the form of potential $U(X)$ as (figure 4)

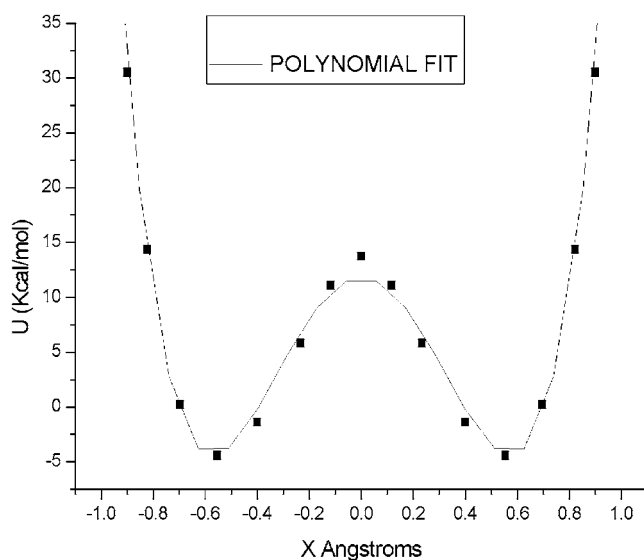$$U(X) = B_0 + B_p X^2 + A_p X^4 \tag{2}$$

Figure 4. Plot showing the variation of net hydrogen bond energy of the amino group of GI with its distance from the *ac*-plane.

where $B_0 = 11.83 \pm 0.51$ kcal mol^{-1}, $B_p = -99.55 \pm 3.6$ Å^{-2} kcal mol^{-1} and $A_p = 152.12 \pm 4.5$ Å^{-4} kcal mol^{-1}.

From the results of the above calculation it was concluded that the $-NH_3^+$ group sees a potential barrier of about 16 kcal mol^{-1} (0.69 eV/molecule) as it moves from L to R. In order to get a qualitative estimate of the probability for a bulky group like $-NH_3^+$ to tunnel through this barrier at room temperature (thermal energy $E = 0.03$ eV) this potential barrier (U) was approximated as a rectangular barrier $Ur(X)$ as shown in figure 3(b). The area under the curve $Ur(X)$ for X lying between $\pm a/2$ was kept equal to that under $U(X)$ for X lying between $\pm X_{min}$. The tunnelling probability calculated using the expression for tunnelling through a rectangular barrier came out to be 1/1717, i.e. one out of every 1717 $-NH_3^+$ groups of TGS molecules in the crystal can tunnel through the barrier at a given instant of time; this is not an insignificant number when one sees that a crystal of volume 1 cm^3 has 3×10^{21} molecules of TGS.

5. Classical anharmonic oscillator model for ferroelectric phase transition in TGS

Yositaka Onodera [16] had proposed a unified oscillator model for ferroelectrics in which he considered a ferroelectric to be an assembly of interacting oscillators, each oscillator moving in an anharmonic potential $U(x) = A_p x^4 + B_p x^2$, where x stands for the displacement of an oscillator. A_p was taken to be positive definite, while B_p may be either positive or negative. The Hamiltonian describing this system was

$$H = H_0 + H_1,$$
$$H_0 = (M/2)(dx/dt)^2 + U(x), \tag{3}$$
$$H_1 = -[\gamma \langle x \rangle + E]x$$

where M gave the mass of an oscillator, $\gamma \langle x \rangle x$ represented the interaction between the oscillators and E was an external field (for field free case $E = 0$). This system underwent a

phase transition in both $B_P < 0$ and $B_P > 0$ cases at a Curie temperature T_C determined by γ.

$$T_C = 2\gamma/|B_p|. \tag{4}$$

Here T_C is in units of $B_p^2/4A_p k_B$. The phase transition was considered displacive or order–disorder depending on the value of A_P and B_P, i.e. $B_p > 0$ or $k_B T_C \geqslant B_P^2/4A_P$, displacive; $B_p < 0$ and $k_B T_C \ll B_P^2/4A_P$, order–disorder.

In order to describe the ferroelectric phase transition in TGS this unified oscillator model was used. For TGS the oscillators were the polar $-NH_3^+$ groups of GI, oscillating in a double well ($B_p < 0$) about the mirror plane (MP) perpendicular to the b-axis at temperatures $T > T_C$. Since $B_P^2/4A_P = 16.2$ kcal mol^{-1} was very much greater than $k_B T_C$ (0.63 kcal mol^{-1}), the phase transition at T_C was considered to be order–disorder type. The interaction $\gamma \langle X_{min}^2 \rangle$ (most likely dipolar in nature) between these oscillators caused the phase transition at a T_C.

Using the experimentally obtained value of T_C (322 K) and the potential parameters B_P and A_P, the value of γ for TGS was calculated to be 1.95 kcal mol^{-1} Å^{-2} and the interaction energy $\gamma \langle X_{min}^2 \rangle = 0.60$ kcal mol^{-1} (this agrees well with the thermal energy at T_C, $k_B T_C = 0.63$ kcal mol^{-1}).

In order to calculate the dipolar interaction energy between the polar $-NH_3^+$ groups one needed to know the dipole moment associated with the group. The bond between nitrogen and hydrogen is a polar bond; the value of the dipole moment of this bond is quoted to be 1.3 D in the literature. The $-NH_3^+$ group has three such polar bonds, making an angle of 109° with each other (tetrahedral geometry); the resultant dipole moment of the group was calculated by taking a vector sum of the dipole moments of the individual polar bonds. The magnitude of the dipole moment (p) (hereafter vectors are represented by bold letters) turned out to be 1.44 D and the direction was along the N1–CA1 bond of GI. The dipolar interaction energy of a dipole p_i located at a lattice site i due to all the other dipoles was obtained using the expression for dipolar interaction energy:

$$E_i = 1/4\pi\varepsilon_o \sum_j [p_i p_j - 3(p_i r_{ij})(p_j r_{ij})/r_{ij}^2]/r_{ij}^3. \tag{5}$$

Here the r_{ij} are the displacement vectors between the dipoles p_i and p_j; these were generated using the space group symmetry and cell parameters of the TGS crystal. Value of the dipolar interaction energy turned out to be 0.71 kcal mol^{-1}. This was in good agreement with the value of interaction energy calculated above. Hence, it was concluded that the interaction represented by the term $\gamma \langle X_{min}^2 \rangle$ was the dipolar interaction between the $-NH_3^+$ dipoles; this dipolar interaction between the $-NH_3^+$ dipoles causes the transition at T_C. The unit cell dipole moment due to the $-NH_3^+$ dipoles calculated using the unit cell symmetry was

$$\mu_{cell} = 2p_b b = (1.21b)D$$

where p_b is the component of p along the b-axis and b is a unit vector along the b-axis.

Gonzalo *et al* [17–20] had described the transition mechanism in crystals belonging to TGS family with an Ising-type theoretical model in which they considered the unit cell to possess a dipole moment μ_{cell} that had two orientation states. Without looking into the microscopic origin of μ_{cell}, using only the dielectric data, Gonzalo [19] was able to predict the value of dipole moment $\mu_{cell} \sim \kappa P_{so} V_c = 1.39$ D, where V_c is the unit cell volume, P_{so} is the saturation polarization and $P_d = \kappa P_{so}$ gives the relation between the saturation polarization P_{so} and the dipolar polarization P_d. This value compared well with the unit cell dipole moment $\mu_{cell} = 1.21$ D calculated using the dipole moments of the $-NH_3^+$ group of GI. Hence it was concluded that the elementary dipole moment referred to by Gonzalo was the $-NH_3^+$ dipole moment and the two orientation states of this dipole corresponded to the two equivalent positions of $-NH_3^+$.
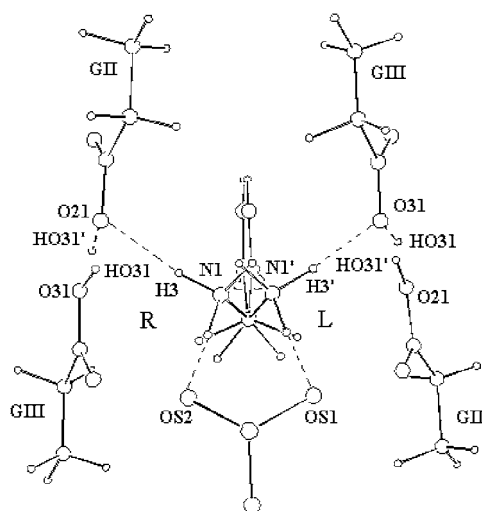
Figure 5. Correlation between the amino group position and hydrogen position for the GII–H–GIII hydrogen bond.

6. Correlation between $-NH_3^+$ flipping and proton switching in the GII–H–GIII hydrogen bond

According to studies conducted by Ramanadham *et al* [21], the oxygen atom covalently bonded to the hydrogen atom in a neutral carboxyl group (–COOH) cannot act as an acceptor of a hydrogen bond, as it has no valence left for the formation of the bond. This result was obtained using the bond valence theory given by Brown [22]; it is an empirical theory which considers every atom to possesses a valence (v) which is a measure of its bonding powder. This criterion of hydrogen bonding in carboxyl group is often used in protein crystallography where hydrogen positions are not known to establish whether a carboxyl group is ionized or not.

In TGS there exists a hydrogen bond $N1^+$–H3- - -O21 between the $-NH_3^+$ group of GI at position R and the ionized carboxyl group of GII (figure 1). When the polarization reverses, the above-mentioned hydrogen bond is broken and a new hydrogen bond $N1'^+$–H3′- - -O31 between the $-NH_3^+$ group of GI at position L and the carboxyl group of GIII is formed (figure 5). As the carboxyl group oxygen O31 that was covalently bonded to hydrogen HO31 is forced be an acceptor of the hydrogen bond $N1'^+$–H3′- - -O31, the hydrogen HO31 is pushed to a new location HO31′ (ionizing the carboxyl group of GIII), so as to satisfy the above-mentioned criteria of hydrogen bonding in the carboxyl group. The hydrogen bond between GII and GIII that was earlier O31–HO31- - -O21 becomes O31- - -HO31′–O21 (figure 5). GIII in this case becomes zwitterionic (dipolar) in nature and GII becomes monopolar. Hence it was concluded that the swing of the amino group of GI between R and L positions is coupled to the hydrogen atom movement (figure 5) in the GII–H–GIII hydrogen bond through the hydrogen bonds $N1^+$–H3- - -O21 and $N1'^+$–H3′- - -O31 between the amino group at R and L positions and the carboxyl group of GII and GIII respectively.

Dielectric spectroscopic studies conducted by Petzelt *et al* [23] indicated that the well known critical relaxation represented by a frequency γ_1' ($\gamma_1' = A'(T_C - T) = 0.8$ cm^{-1} at $T = 303$ K, $A' = 0.035$ cm^{-1}) in TGS was coupled to another inactive soft relaxation ($\gamma_2' = 0.2$ cm^{-1}) through a coupling constant $|\alpha'| = 0.4$ cm^{-1}; soft relaxation γ_1' bears the

whole dipole moment and is temperature dependent. The relaxation frequency γ_1' should be attributed to the flipping $-NH_3^+$ group of GI because as mentioned in the section above almost the whole of the dipole moment of the unit cell (μ_{cell}) can be attributed to this group, and the phase transition at T_C can be described almost entirely by the dynamics of this group. The inactive soft relaxation γ_2' can be associated with the flipping of the hydrogen in the hydrogen bond GII–H–GIII, which is coupled to the $-NH_3^+$ group of GI through a hydrogen bond as described above. The GII–H–GIII hydrogen bond lies almost entirely along the crystallographic c-axis and hence an AC field applied along the polar b-direction does not interact with the dipole moment associated with this hydrogen bond (as the dipolar interaction energy is $\boldsymbol{p} \cdot \boldsymbol{E}$) and as a result this relaxation mode is inactive.

7. Conclusions

Starting from the available structural information on TGS in its ferroelectric and paraelectric phases the double-minimum potential seen by the amino group of glycine GI in TGS was successfully modelled using the potential function for bent hydrogen bonds; the ferroelectric phase transition in TGS was interpreted in terms of the dipolar interaction energy between the amino groups. It was established that the ferroelectric phase transition in TGS takes place due to the existence of two competing forces within the crystal: on one hand the dipolar interactions between the $-NH_3^+$ dipole moments tend to bring in an ordered state; on the other hand the thermal energy of the crystal tends to bring in a disordered state. At the transition point T_C the dipolar interaction energy leading to an ordered state is equal to the thermal disordering energy $k_B T_C$; for $T < T_C$ dipolar ordering is dominant whereas for $T > T_C$ thermal disorder takes over. This interpretation of the phase transition can also explain the decrease in T_C when a bigger selenate group ($-SeO_4^{2-}$) replaces the sulfate group (SO_4^{2-}) in the isomorphous compound triglycine selenate (TGSe) [9]. The distance between the interacting dipoles increases due to the increase in the unit cell dimensions in TGSe; this leads to a decrease in the value of dipolar interaction energy (E_i) of the dipoles since $E_i \propto 1/r^3$; as a result the transition temperature decreases. Similarly, the increase in T_C with increase in pressure [1] can be explained. The decrease in the distance between the interacting dipoles with pressure results in an increase in the dipolar interaction energy between them, leading to an increase in T_C.

It was concluded that the swinging of the amino group of GI in TGS is coupled to the proton motion in the GII–H–GIII bond through a hydrogen bond. This hydrogen bond when formed pushes the hydrogen in the GII–H–GIII bond to occupy a position such the valences of the carboxyl groups of both GII and GIII are satisfied.

References

[1] Jona F and Shirane G 1962 *Ferroelectric Crystals* (Oxford: Pergamon) ch 2
[2] Kaneko N, Takahashi H and Higasi K 1974 *Bull. Chem. Soc. Japan* **47** 1148
[3] Slosarek G, Heuer A, Zimmermann H and Haeberlen U 1989 *J. Phys.: Condens. Matter* **1** 5931–54
[4] Kay M I and Kleinberg R 1973 *Ferroelectrics* **5** 45–52
[5] Lock P J 1971 *Appl. Phys. Lett.* **19** 390–1
[6] Hofmann G, Neumann N and Budzier H 1992 *Ferroelectrics* **133** 41–5
[7] Itoh K and Mitsui T 1973 *Ferroelectrics* **5** 235–51
[8] Keve E T, Bye K L, Whipps P W and Annis A D 1971 *Ferroelectrics* **3** 39–48
[9] Stankowski J 1981 *Phys. Rep.* **77** 1–46
[10] McMahon M I, Nelmes R J, Kuhs W F, Dorwarth R, Plltz R O and Tun Z 1990 *Nature Lett.* **348** 317–19
[11] Robertson G N and Lawrence M C 1981 *J. Phys. C: Solid State Phys.* **14** 4550–74

[12] Kaneko N, Takahashi H and Higasi K 1977 *J Phys. Chem. Solids* **38** 849–53
[13] Chidambaram R and Sikka S K 1968 *J. Chem. Phys. Lett.* **2** 162
[14] Chidambaram R, Balasubramanian R and Ramachandran G N 1970 *Biochim. Biophys. Acta* **221** 182–95
[15] Ramanadham M and Chidambaram R 1978 *Advances in Crystallography* ed R Srinivasan (New Delhi: Oxford–IBH) pp 81–103
[16] Onodera Y 1970 *Prog. Theor. Phys.* **44** 1477–99
[17] Gonzalo J A and Lopez-Alonso J R 1964 *J. Phys. Chem. Solids* **25** 303–10
[18] Gonzalo J A 1970 *Phys. Rev.* B **1** 3125–31
[19] Gonzalo J A 1974 *Phys. Rev.* B **9** 3149–51
[20] Lorenzo J E, Martinez J L and Gonzalo J A 1988 *Ferroelectrics* **88** 101–9
[21] Ramanadham M, Jakkal V S and Chidambaram R 1993 *FEBS* **323** 203–6
[22] Brown I D 1981 *Structure and Bonding in Crystals* vol 2 (New York: Academic) pp 2–30
[23] Petzelt J, Kozlov G V and Volkov A A 1987 *Ferroelectrics* **73** 101–23